

PANSI XIE^{1,2}, BAOFU HUANG^{1,2*}, YONGPING WU^{1,2}, SHENGHU LUO^{2,3},
TONG WANG^{1,2}, ZHUANGZHUANG YAN^{1,2}, JIANJIE CHEN⁴

DIP-ANGLE-EFFECT-BASED DEFORMATION AND FAILURE LAW OF STEEPLY DIPPING STOPE ROOFS WITH LARGE MINING HEIGHTS

The deformation and failure law of stope roofs is more complicated than horizontal coal seams affected by the angle of the coal seam during the mining process of steeply dipping coal seams. This study focused on and analysed the working face of a 2130 coal mine with steep dipping and large mining height. Through the use of numerical calculation, theoretical analysis, physical similar material simulation experiments, and field monitoring, the distribution characteristics of roof stress, as well as the three-dimensional caving migration and filling law, in large mining height working faces under the dip angle effect was investigated. The influence mechanism of the dip angle change on the roof stability of large mining heights was investigated. The results revealed that the roof stress was asymmetrically distributed along the inclination under the action of the dip angle, which resulted in roof deformation asymmetry. With the increase in the dip angle, the rolling and sliding characteristics of roof-broken rock blocks were more obvious. The length of the gangue support area increased, the unbalanced constraint effect of the filling gangue on the roof along the dip and strike was enhanced, and the height of the caving zone decreased. The stability of the roof in the lower inclined area of the working face was enhanced, the failure range of the roof migrated upward, and the damage degree of the roof in the middle and upper areas increased. Furthermore, cross-layer, large-scale, and asymmetric spatial ladder rock structures formed easily. The broken main roof formed an anti-dip pile structure, and sliding and deformation instability occurred, which resulted in impact pressure. This phenomenon resulted in the dumping and sliding of the support. The 'support-surrounding rock' system was prone to dynamic instability and caused disasters in the surrounding rock. The field measurement results verified the report and provided critical theoretical support for field engineering in practice.

Keywords: Steeply dipping coal seam; large mining height working face; dip angle effect; stability control of the roof; support-surrounding rock

¹ XI'AN UNIVERSITY OF SCIENCE AND TECHNOLOGY, SCHOOL OF ENERGY ENGINEERING, XI'AN 710054, CHINA

² XI'AN UNIVERSITY OF SCIENCE AND TECHNOLOGY, KEY LABORATORY OF WESTERN MINE EXPLOITATION AND HAZARD PREVENTION MINISTRY OF EDUCATION, XI'AN 710054, CHINA

³ XI'AN UNIVERSITY OF SCIENCE AND TECHNOLOGY, DEPARTMENT OF MECHANICS, XI'AN, 710054, CHINA

⁴ XINJIANG COKING COAL GROUP CORPORATION LIMITED, XINJIANG 830025, CHINA

* Corresponding author: 3251403264@qq.com



© 2023. The Author(s). This is an open-access article distributed under the terms of the Creative Commons Attribution-NonCommercial License (CC BY-NC 4.0, <https://creativecommons.org/licenses/by-nc/4.0/deed.en>) which permits the use, redistribution of the material in any medium or format, transforming and building upon the material, provided that the article is properly cited, the use is noncommercial, and no modifications or adaptations are made.

1. Introduction

Mining in steeply dipping coal seams with a dip angle of 35° - 55° is difficult [1,2]. However, more than 50% of steeply dipping coal seams are high-quality coking coal and anthracite, which are rare coals for protective mining in China. Most such seams are thick. Large mining heights (3.5-5.0 m thick) can considerably improve resource mining efficiency [3,4]. The stability control of the 'roof-support-floor' (R-S-F) system, especially the roof, is critical for the safe and efficient mining of the working face in steeply dipping coal seams [5-8].

The mine pressure behaviour law [9-13], roof spatial structure and its loading mechanism [14,15], asymmetric deformation and failure law of roof strata [16-18], stress transfer path and evolution mechanism [19-20], main roof fracture mode and evolution process [21,22], interaction law between surrounding rock migration and support [23-26], stope gangue slip filling effect, and overlying rock movement mechanism [27,28] under various mining conditions of steeply dipping coal seams have been studied through theoretical analyses, field measurements, and numerical calculations. The results of these studies have laid the foundation for mining theory and technology of steeply dipping coal seam. The coal seam dip angle is the main factor of surrounding rock control in steeply dipping seam mining. In the mining of coal seam with steep dipping and large mining height, because of the influence of the dip angle, the caving gangue slides along the inclined working face, and the goaf exhibits non uniform filling, which results in the asymmetric characteristics of strata behaviour law, roof deformation and failure characteristics, and the spatial form of the roof structure.

Based on the existing research work, this paper takes the working face of steeply dipping and large mining height in Xinjiang 2130 coal mine as the engineering background, using physical similar material simulation experiments and theoretical analysis to study the deformation and failure characteristics of the roof of steeply dipping and large mining height under the action of gangue filling. Numerical calculations were performed to analyse the distribution characteristics of roof stress of the working face with steeply dipping and large mining heights under various working face dip angles, as well as the three-dimensional space caving migration and filling law of the stope roof. Through field monitoring, the pressure law of the roof, the load characteristics of support, and the nonuniform filling characteristics of gangue were analysed to confirm the accuracy of numerical calculations and theoretical derivations. The results of this study can considerably advance the theory and practice of roof stability control in the working face of steeply dipping coal seams.

2. Engineering background

Xinjiang Coking Coal Group 2130 coal mining 5# coal seam. The average thickness is 5 m, the average dip angle is 45° , the bulk density is 1.35 t/m^3 , and the hardness coefficient $f=0.3$ - 0.5 . The immediate roof is gravelly coarse sandstone of thickness 2.4 m. The main roof is medium sandstone of thickness 16.2 m. The floor is coarse sandstone with a thickness of 17 m. The coal seam roof and floor histogram are shown in Fig. 1. The inclined length is 100 m, and the strike length is 1766 m. The comprehensive mechanised large mining height method is adopted. The mining height is 4.5 m, and the roof is managed by all caving methods.





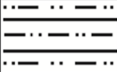
Layers	Histogram	Thickness / m	lithological description
Main roof		16.2	Gray white sandstone, quartz-based
Immediate roof		2.4	Gray-white pebbly coarse sandstone
Coal seam		5.0	Containing 3 layers of dirt band
Immediate floor		0.8	Gray black, mainly quartz
Main floor		17	Coarse sandstone, joint development

Fig. 1. Coal seam roof and floor histogram

3. Physical similar material experiment

According to the measured physical and mechanical parameters of working face and laboratory rock mechanics experiments, river sand was used as the aggregate, and gypsum and calcium carbonate were the cementing materials. The ratio of similar materials in the physical model is presented in TABLE 1. The simulation material is paved on a three-dimensional loading test bench. After paving, compaction, and random characterisation of joints, mica was used to simulate stratification. The geometric similarity constant of the physical model was 20, the bulk density similarity constant was 1.6, the stress similarity constant was 32, and the time similarity constant was 201/2. The self-developed hydraulic support model was used in the experiment, and the data acquisition box and computer terminal were used to receive and process the sensor signals. The camera took photos to record the roof fracture form, rock-hinged structure and caving gangue accumulation form. The physical similarity model of the pavement is displayed in Fig. 2.

TABLE 1

Ratio of similar materials

Rock formation	Lithology	Strata thickness/m	Model thickness/cm	Ratio (river sand : gypsum : calcium carbonate : coal dust)
Main roof	Medium sandstone	16.2	81.0	837
immediate roof	gravelly coarse sandstone	2.4	12.0	846
Coal seam	5# coal	5	25.0	20 : 1 : 3 : 15
Immediate floor	Carbon mudstone	0.8	4.0	828
Main floor	Coarse sandstone	17	85.0	846

Fig. 3 displays the failure and migration characteristics of surrounding rock in steeply dipping and large-height coal seam mining. The movement process of roof strata was mainly bending subsidence → layer separation → fracture caving → sliding filling.

The failure and migration characteristics of the stope roof were more active than those of general mining height in the steeply dipping coal seam. With the increase in the mining height, the space of roof caving and migration increased. After the support was moved, the immediate

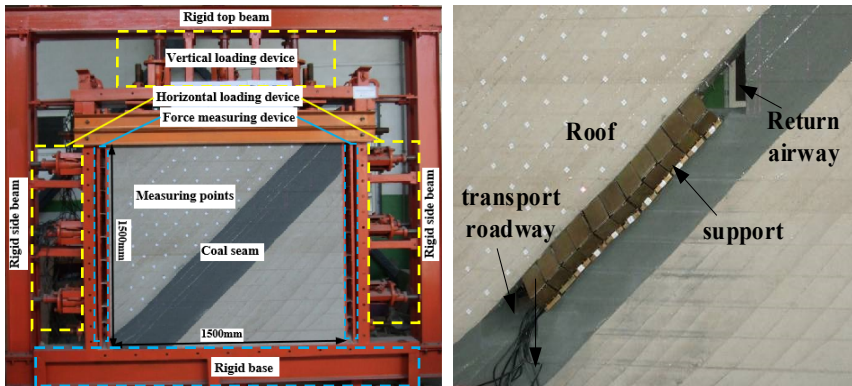


Fig. 2. Physical similar material model

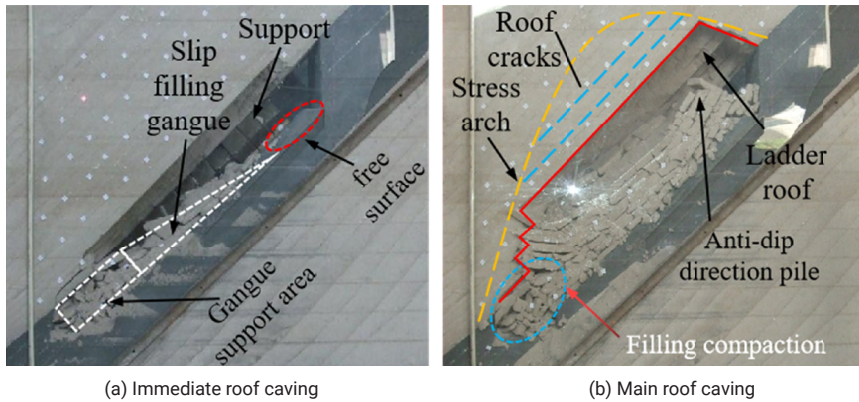


Fig. 3. Roof cave-filling evolution characteristics

roof of the middle and upper areas broke and fell first, and along the floor slides and filled to the inclined lower area, which formed the rectangular gangue support area and the free surface area along the inclination direction, as displayed in Fig. 3(a).

With the advance of the working face, the main roof strata were destroyed, caved, and slipped to form a layered accumulation. The filling compaction degree of the inclined lower part was the highest, and the middle and upper parts were partially filled. Unfilled space was observed in the inclined upper part. In the area of the uncaving immediate roof and main roof strata, an obvious ladder-like contour was formed because of the large migration space. On the dip section, this contour exhibited multilevel ladder-like characteristics of lower inclined and higher middle-upper layers. In the upper part of the main roof, the roof cracks are produced, and the rock layer produced by the cracks does not have the bearing capacity. Therefore, a load-bearing arch is formed with the vault in the upper part of the working face, the upper arch foot on the return airway side, and the lower arch foot on the transport roadway side, as displayed in Fig. 3(b).

The movement space of the roof in the inclined lower area was limited, and the caving was not sufficient. The adjacent rock blocks in this range were hinged and extruded from each

other to form a stable dip-direction pile structure. The middle and upper part of the inclination was structurally active; the roof strata moved actively and exhibited a large migration space. After the main roof was broken, a rotating and anti-dip direction pile structure formed easily; the instability of the structure formed impact pressure on the area (Fig. 3(b)). During the experiment, the lateral load of the lower and middle supports of the working face was stable, whereas the upper support load was extremely unstable, and was vulnerable to the impact load of the roof (Fig. 4,5). The support and surrounding rock had a weak contact relationship, resulting in partial load, empty load, and extrusion between the support. This made it challenging to control the stability of the support, leading to dynamic instability and rock disasters. Additionally, gas tended to accumulate in the upper corner of the caved area, significantly affecting the safety of mining operations on the working face.

4. Mechanical analysis of the inclined roof rock beam

The mechanical model of the inclined roof rock beam was established according to the nonuniformity characteristics of caved gangue sliding filling in the inclined direction of the work-

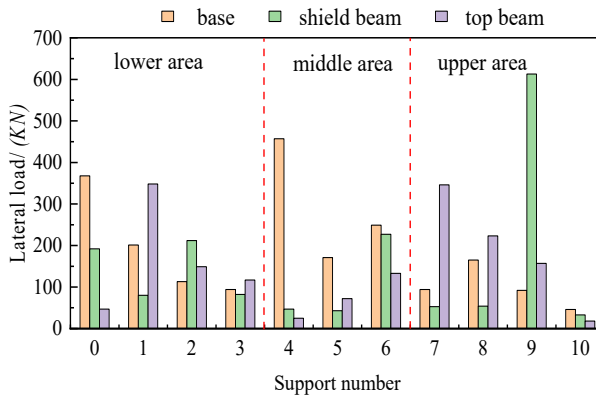


Fig. 4. Distribution characteristics of lateral load of supports



Fig. 5. Characteristics of interaction between supports

ing face, as displayed in Fig. 6. Here, α is the coal seam dip angle, °; L is the inclined length of working face, m; a is the inclined length of the gangue support area, m; $q(x)$ is the normal load of rock beam, kN/m; P_A is the load at section A, kN/m; γ is bulk density, kN/m³; the action load of overlying strata on the main roof beam can be calculated using the following expression:

$$q(x) = (P_A - x\gamma \sin \alpha) \cos \alpha \quad (1)$$

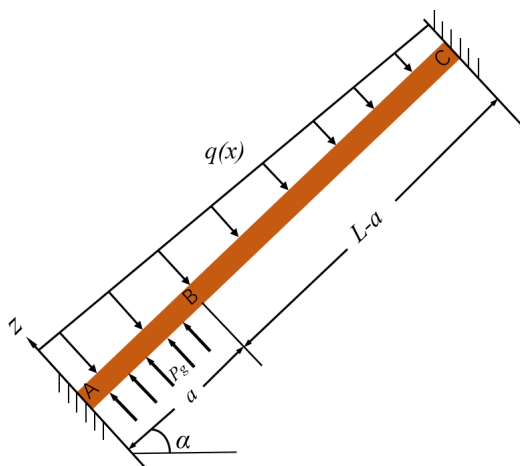


Fig. 6. Mechanical model of the inclined roof rock beam

As displayed in Fig. 7(a), the AB section rock beam, the deflection differential equation can be expressed as follows:

$$EI \frac{d^2 z_1(x)}{dx^2} = -M_a - F_a x + \int_0^x q(\delta)(x - \delta) d\delta - P_g \frac{x^2}{2} \quad (2)$$

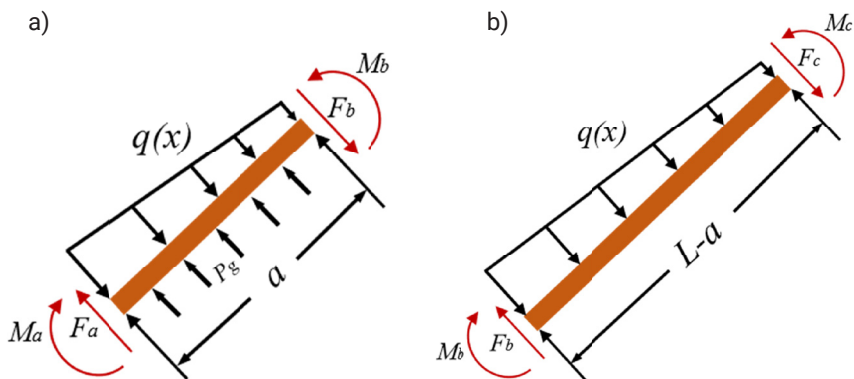


Fig. 7. Mechanical analysis of deformation and failure of the inclined roof rock beam:
 a) Rock beam in the gangue supporting area, b) Rock beam in the unsupported area of gangue

As detailed in Fig. 7(b), the BC section rock beam, the deflection differential equation can be expressed as follows:

$$EI \frac{d^2 z_2(x)}{dx^2} = -M_b - F_b(x-a) + \int_a^x q(\delta)(x-\delta)d\delta \quad (3)$$

M_b and M_c are the bending moments respectively, and F_b and F_c are the shear forces respectively.

$$M_a + F_b a + \int_0^a q(x)xdx - P_g a \frac{a}{2} - M_b = 0 \quad (4)$$

$$F_a - F_b + P_g a + \int_0^a q(x)dx = 0 \quad (5)$$

where A_2, B_2, A_3, B_3, M_b , and F_b are coefficients. According to the continuity conditions of A, B , and C sections of rock beams, the following expressions can be obtained:

$$z_1(0) = 0, z_1'(0) = 0 \quad (6)$$

$$z_2(L) = 0, z_2'(L) = 0 \quad (7)$$

$$z_1(a) = z_2(a), z_1'(a) = z_2'(a) \quad (8)$$

Furthermore, $z_1(x)$ is the deflection of rock beam:

$$z_1(x) = \frac{1}{120EI} \left[\begin{array}{l} -\cos \alpha x^4 (\sin \alpha \gamma x - 5P_A) - 5P_g x^4 - 20F_a x^3 \\ -60M_a x^2 + 120A_1 x EI + 120B_1 EI \end{array} \right] \quad (9)$$

where $z_2(x)$ is the deflection of rock beam:

$$z_2(x) = -\frac{1}{12EI} \left(\begin{array}{l} \gamma \sin(2\alpha) a^3 x^2 - \frac{\gamma \sin(2\alpha) a^2 x^3}{2} + \frac{\gamma x^5 \sin(2\alpha)}{20} \\ -3 \cos \alpha P_A a^2 x^2 + 2 \cos \alpha P_A a x^3 - \frac{P_A \cos \alpha x^4}{2} \\ -6F_b a x^2 + 2F_b x^3 + 6M_b x^2 \end{array} \right) + A_3 x + B_3 \quad (10)$$

Combined with the deflection equations (9) and (10) of the rock beam, the breaking deformation law of the rock beam under various dip angles can be determined.

Fig. 8 reveals that because of the dip angle effect, roof deformation exhibits asymmetric characteristics. With the increase in the dip angle, the normal load component of overlying strata decreased, and the deflection of the rock beam decreased gradually. The peak position of deflection shifted from the middle to the middle-upper layer. The filling of the gangue changed the stress and constraint conditions of the roof. The caving gangue was filled down to the lower goaf, and the gangue filling area length increased. The lower area roof stability enhancement and the vulnerable position moves to the middle-upper. The stability of the middle-upper parts is reduced,

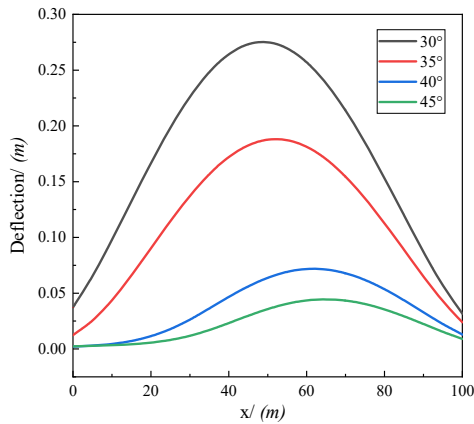


Fig. 8. Deflection diagram of rock beam under various dip angles

and it is prone to slip and deformation instability. The impact pressure is formed, resulting in the dumping and sliding of the support, and the dynamic instability of the support-surrounding rock system induces the disaster of surrounding rock in the working face.

5. Numerical calculation

5.1. Three-dimensional numerical calculation model

The mechanical parameters of coal rocks are determined by field geological surveys and rock mechanics experiments (TABLE 2). The three-dimensional numerical model was established by using the FLAC3D finite element and 3DEC discrete element numerical calculation software (Fig. 9). The working face advanced along the y-axis, and the vertical load of 2MPa was applied to the top of the model to simulate the formation depth of 80 m. The vertical displacement constraint was applied to the bottom of the model, and the horizontal displacement constraint was applied to the front, back, left and right of the model, respectively. The stability characteristics of the large mining height working face roof and the three-dimensional caving migration and filling law of the stope roof were calculated for dip angles 30°, 35°, 40°, and 45°. The Mohr-Coulomb constitutive model was used for calculation.

TABLE2

Mechanical parameters of coal rocks

Lithology	Density (kg/m ³)	Elastic modulus (GPa)	Poisson ratio	Tensile strength/MPa	Cohesion/MPa	Friction angle/(°)
Carbon mudstone	1500	2	0.35	1.1	0.8	23
Coal seam	1350	3	0.30	2.0	1.6	28
gravelly coarse sandstone	2662	2	0.26	1.1	0.8	23
Medium sandstone	2675	1.2	0.31	0.9	1.0	25
Coarse sandstone	2492	20	0.21	1.8	3.1	35

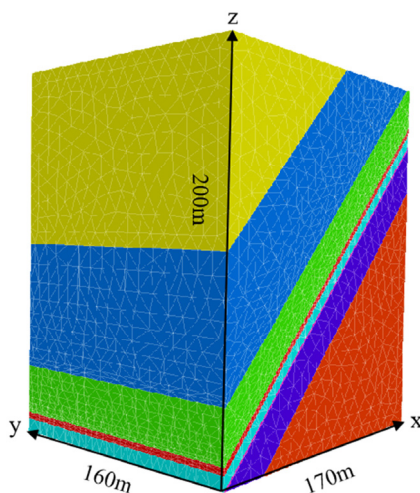


Fig. 9. Numerical analysis model

5.2. Evolution characteristics of roof stress

Fig. 10 reveals that along the working face inclination, an asymmetric arch stress release zone is formed in the roof and floor strata, and the minimum vertical stress is 0.08-1.08 MPa. The stress concentration zone was formed in the upper and lower ends, and the maximum concentration stress was 9.1-9.4 MPa. Due to the dip angle of the coal seam, the stress distribution exhibited asymmetric and local regional characteristics. The stress release area of the roof in the middle and upper part was larger than that in the lower part, and the pressure relief range was an 'inverted spoon'. The pressure relief height of the middle upper was the largest. The peak value of concentrated stress in the lower end of the working face was greater than that in the upper-end area. The upper roof was in a positive stress state and vulnerable to tensile failure. The lower roof was in a negative stress state and prone to compression failure. With the increase in the dip angle, the height and width of the roof stress relief arch gradually reduced, and the arch axis shifted to the upper part. The concentrated stress value and influence range of the upper and lower ends of the coal body gradually reduced, and the asymmetric and regional characteristics of the stress release zone became clear.

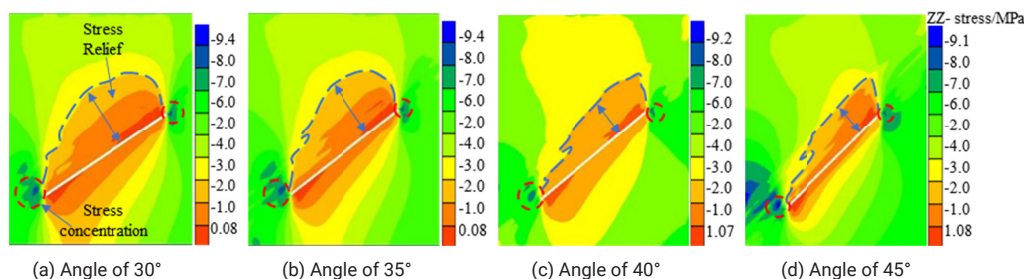


Fig. 10. Vertical stress distribution along inclined under various dip angles

Along the strike, the vertical stress of the surrounding rock of stope was redistributed, and the roof and floor strata formed a symmetrical arch stress release zone. The roof stress relief zone was larger than the floor, and the minimum vertical stress was 0.03-1.2 MPa. The stress concentration zone formed in the front and rear coal walls, and the maximum concentration stress was 8.2-8.6 MPa. Under various dip angles, the stress distribution characteristics of the working face were the same, and the pressure relief height in the central region was the largest. With the increase in the dip angle, the vertical stress of the roof increased, and the peak value of concentrated stress on both sides decreased, including the stress arch height (Fig. 11).

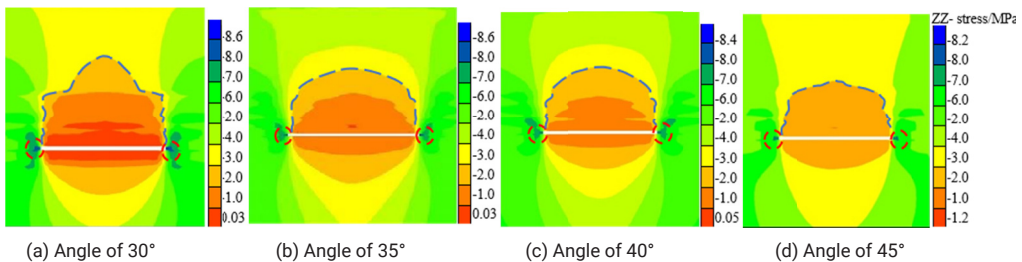


Fig. 11. Vertical stress distribution along strike under various dip angles

5.3. Roof caving migration filling characteristics

In the mining of the coal seam with steeply dipping and large mining height, the deformation failure and filling form of surrounding rock exhibited obvious asymmetric characteristics. The roof strata collapse exhibited a unique ‘multi-stage ladder key layer’ roof structure with the low lower and high upper layers of the working face. The low-level ladder structure was located in the lower part of the working face, and the horizon was low, mainly in the immediate roof strata. The weighting strength was small, and the step was large, which affects the stability of the surrounding rock in the lower area of the working face. The high-level ladder rock structure was located in the middle and upper parts, which was mainly composed of main roof strata with high horizon, strong weighting strength, small step, short period and impact. Furthermore, the vertical distance from the stope floor was the largest, which plays a key role in roof stability. The broken rock strata existed in the form of inclined stacking. The broken rock blocks in the lower inclined region formed hinged structures, accompanied by reverse rotation, and were mainly dip pile structures. In the middle and upper regions, the dip pile structure and anti-dip pile structure coexist. When the dip angles of the working face were 30°, 35°, 40°, and 45°, the heights of the roof caving zone were 33.2, 29.6, 26.2, and 23.2 m, respectively. The filling lengths of the caving gangue were 97.5, 83.2, 62.7, and 56.2 m, respectively. With the increase in the dip angle, the filling length decreased gradually, the length of the gangue support area increased, and the filling shape of the inclined section of the accumulated gangue changed. The filling compactness increased from trapezoid → triangle → rectangle + triangle. The degree of filling density increased, and the non-equilibrium constraint characteristics of the roof became more clear. The stability of the roof in the lower part of the tendency is enhanced, and the movement amplitude and activity of the roof strata in the middle and upper parts are increased. The main roof strata are prone to sliding, deformation and instability, forming an anti-dip direction pile.

The structure is unstable and prone to instability forming an impact. The height of the caving zone decreased gradually, and the deformation and failure area developed on the upper part of the working face, as displayed in Fig. 12.

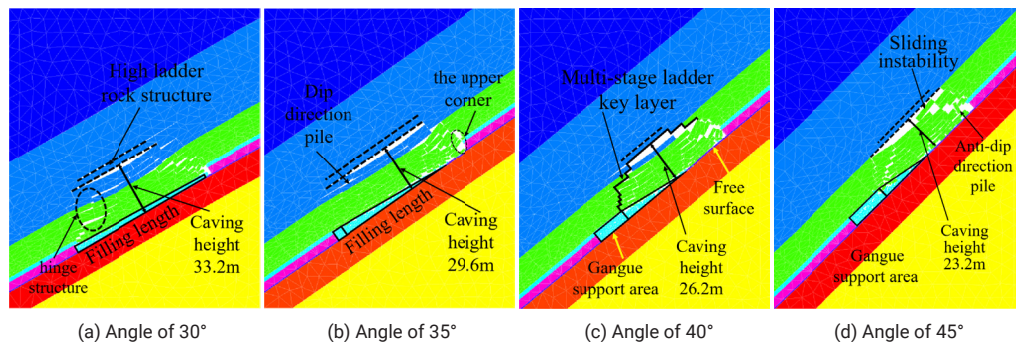


Fig. 12. Caving migration and filling characteristics of roof along inclined under different dip angles

The immediate roof fell with the strike, and after the main roof was broken, considerable cutting and rotation were performed. The broken main roof and the unbroken roof were hinged to form a ‘masonry beam’ structure. The broken main roof rock blocks were hinged and extruded to maintain stability, which formed an inclined masonry structure. The roof strata fell in the symmetrical arch structure. The vault was located in the middle of the strike. The front arch foot was located in the coal wall in front of the working face, and the rear arch foot was located in the coal wall at the open-off cut. When the dip angles of the working face were 30°, 35°, 40°, and 45°, the vault heights were 38.3, 35.5, 33.2, and 31.3 m, respectively. With the increase in the dip angle, the roof failure range gradually reduced, the height and width of the symmetrical arch continuously reduced, and the stability of the surrounding rock strike structure was enhanced, as displayed in Fig. 13.

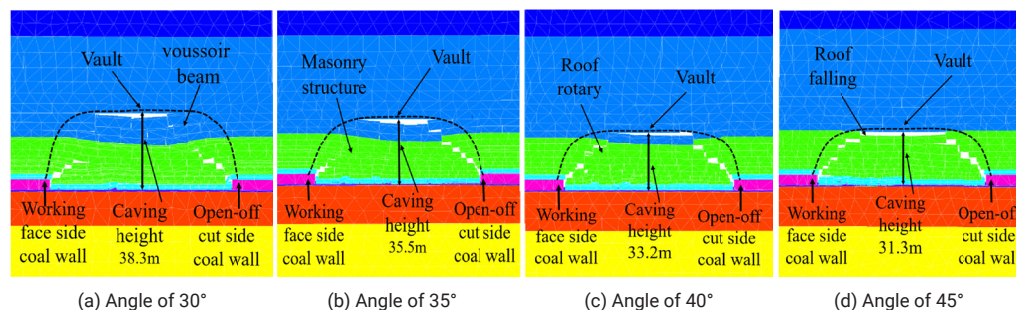


Fig. 13. Caving migration and filling characteristics of roof along strike under various dip angles

The broken immediate roof rock block not only slid down and filled along inclination, but also along the lateral slide. The broken rock block rolls and slides along the coal wall of the

open cut side, and produces a depression area at a certain angle. The accumulation of the upper boundary of the caved gangue-filling body resulted in an asymmetric V-shaped structure along the inclination. From the bottom to the top, the distance between the roof caving gangue and the support increased, which resulted in the filling characteristics of gangue in goaf not only exhibiting obvious asymmetry in the inclination direction but also anisotropy in the advancing direction. With the increase in the dip angle, the inclined component of gravity of caved gangue increased, the degree of rolling and filling increased, the range of the free surface area increased, and the nonuniform characteristics of gangue filling in goaf became significant. The three-dimensional nonequilibrium constraint effect of the filling body on the roof and floor strata along the inclination and advancing direction was obvious, as displayed in Fig. 14.

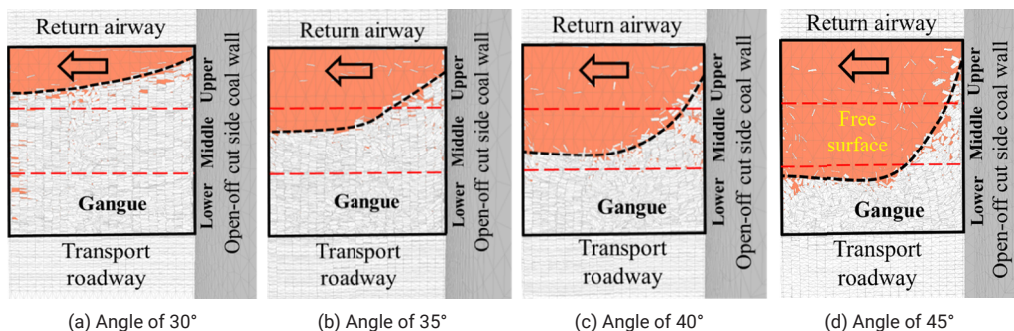


Fig. 14. Deformation and failure characteristics of immediate roof under various dip angles

Because of the three-dimensional nonequilibrium constraint effect of caving gangue, the main roof strata asymmetrically broke, caved, settled, and accumulated. The broken main roof exhibited an obvious hinged structure along the inclination and strike. The initial caving formed ellipsoid caving in the middle and upper areas; periodic caving exhibited a periodic arc rock strip structure. Numerous shear and tensile failure zones were formed in the middle and upper area, mainly vertical settlement, accompanied by lateral displacement and inclination slide. The lower strata's tensile failure zone was limited, resulting in only minor lateral displacement and minimal vertical settlement. Thus, the sequence, upper area settlement > middle area settlement > lower area settlement, was observed. After the initial weighting, the broken main roof and the unbroken rock layer formed a hinged structure, which supported and limited the broken structure under periodic weighting. The main roof exhibited ladder dislocation in various periods along the advancing direction.

The non-uniform filling of gangue leads to the full caving of the middle and upper roof in the working face. Arc triangular block appeared at the upper end, which reduced the restraint of the gangue, resulting in the occurrence of a tensile-shear fracture with a small area and a large rotational subsidence displacement. The arc triangular block at the lower end was carried by the gangue and resulted in a restraint effect on the roof of the overlying stratum, as displayed in Fig. 15(b), with a large area and a small subsidence displacement, resulting in various weighting steps of the upper and lower ends in the process of advancing the working face. The following sequence was observed: the weighting step of the lower end > the middle area > the upper end. The weighting phenomenon in the upper-end area was apparent. The upper caving area partially

exceeded the outside of the return airway, and a trend of upward development was observed. The upper-end rock block was prone to caving and sliding, and formed a ‘cavity’, as displayed in Fig. 15(c). Thus, this phenomenon indicates that when the support is not connected to the roof, sliding or dumping of the support may occur. With the increase in the dip angle, the space, amplitude, and intensity of roof-caving rock movement in the middle and upper regions increased considerably, and the basic form of surrounding rock structure formed after failure along the inclination and advancing direction differed considerably.

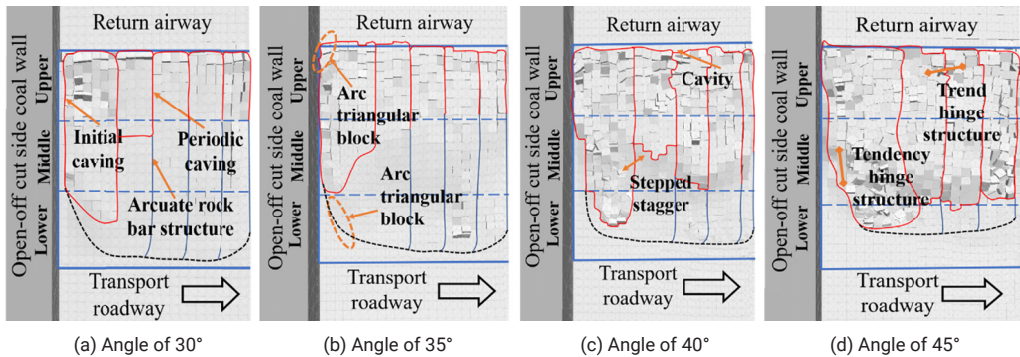


Fig. 15. Deformation and failure characteristics of main roof under various dip angles

6. Field monitoring

To investigate the deformation, failure and migration characteristics of surrounding rock in the mining process, and the adaptability of supporting equipment, the measuring areas were arranged along the upper, middle, and lower three regions. The KJ377 mine pressure dynamic monitor was used to continuously record the load on the support in the measuring area and then analyse the behaviour law of the mine pressure in the working face and the stress characteristics and stability characteristics of the support in various areas.

The field monitoring results revealed that along the inclined direction, the mine pressure law revealed the characteristics of unbalanced sub-regions. The average working resistance of the support in the upper, middle, and lower parts of the working face was approximately 5186, 6355, and 3862 kN. Thus, the working resistance (support load) in the middle area is the highest, followed by the upper area, whereas that in the lower area was the lowest. The working resistance of the lower area was approximately 60.7% of the middle area, and the working resistance of the upper area was approximately 81.6% of the middle area. A large-scale empty roof area existed in the upper inclined area, which formed a cross-layer, large-scale, asymmetric spatial ladder residual wall roof rock structure (Fig. 17). This corresponds to the deformation and failure characteristics of the surrounding rock in the numerical calculation part. The periodic instability of the ladder structure considerably affects gangue caving and filling and the stability of the support and coal wall.

The stability of the support surrounding the rock system differs in various areas of the working face. The support changed considerably in the middle and upper areas, whilst the working resistance of some supports was small or even close to zero (Fig. 16), which resulted in inadequate

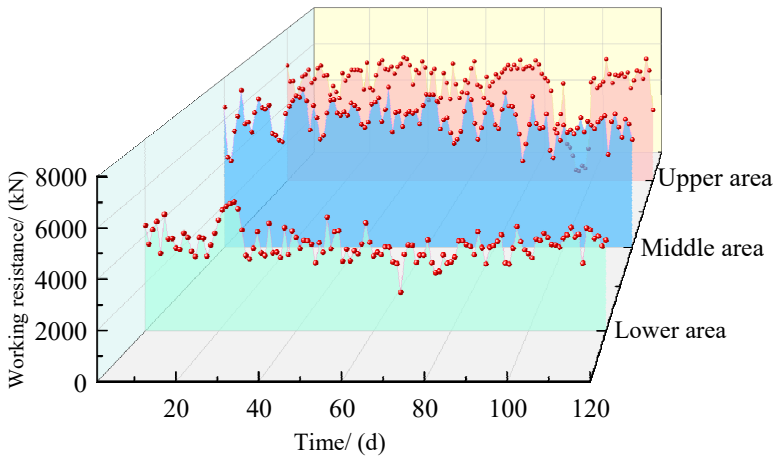


Fig. 16. Characteristic of the working resistance in various areas of the working face

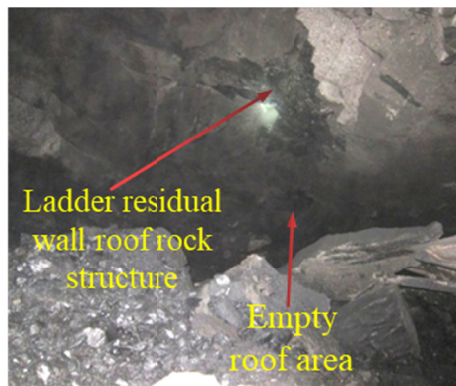


Fig. 17. Field observation results (Angle of view: upper corner of return airway)

R-S-F system elements, which are prone to roof caving. In the upper and middle regions, the load of individual supports exceeded the rated working resistance, and the supports push and bite each other. Corresponding to the theoretical analysis part, it shows that the roof in the middle and upper parts is prone to damage, resulting in roof sliding, deformation and instability, causing empty roof, no-load support, toppling between supports, extrusion and other phenomena. The load of the R-S-F system is complex, and its instability tendency is considerably higher than that of gently inclined coal seam mining. As a result of significant weight accumulation, dynamic instability can occur, which can lead to disasters in the surrounding rock.

Therefore, in order to reduce the phenomenon of roof caving and support toppling, we put forward the following prevention and control measures in the mining of large mining height working:

- (1) In the mining of the working face, the working resistance and initial support force of hydraulic support should be set up in different regions. By adjusting the output pressure

of the hydraulic pump station of support system and the safety threshold of support itself, the working resistance of support in the lower region is lower than that in the middle region by 30% ~ 40%, while that in the upper region is lower than that in the middle region by 10% ~ 20%. The initial support force of support should reach about 80% of its working resistance, to prevent the roof from sinking prematurely and reduce the strength of impact load during weighting.

- (2) The hard roof space partition weakening technology of “deep hole pre-splitting of the main roof in the middle of the working face + deep hole roof cutting in the roof of the two roadways” is adopted. Four non-equaling blast holes are arranged in each group in the mining roadway by using the down-the-hole drilling rig, and the non-uniform charge structure and group blasting method are adopted. The advanced periodic blasting weakening treatment of the hard roof with steeply dipping seam and large mining height can reduce the working resistance of the support in the upper, middle and lower parts of the working face, reduce the weighting step, eliminate the large area of the suspended roof and impact dynamic load, and improve the stability of the “support-surrounding rock” system. See Fig. 18.

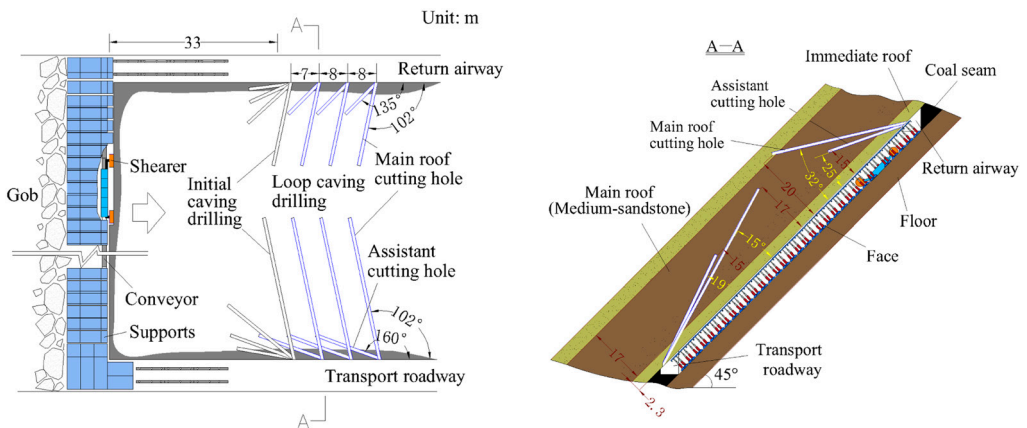


Fig. 18. Hard roof space partition weakening

- (3) The large working resistance support is selected, and a large number of high-strength plates are used to meet the overall strength and stiffness requirements of the support. The weight of the support is reduced, which can not only resist the impact of gangue but also improve the stability of the support. Increase the area of the support base, increase the contact area between the support and floor, and reduce the probability of damage to the floor; the roof beam is completely closed to the roof and has a large front-end support force, which is conducive to the stability of the support and can also effectively prevent roof leakage and spalling. Lifiable blocking gangue plate are set up in front and side of the support, respectively, which can prevent the gangue from rolling down and impacting people; through the retractable connecting device, multiple supports are connected together to form an overall anti-falling and anti-skid unit, and the support toppling and sliding state is adjusted in real-time. See Fig. 19.

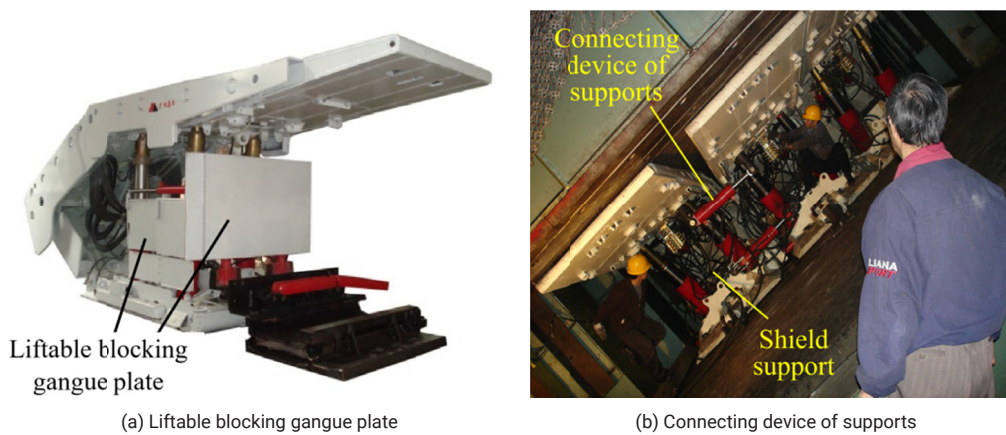


Fig. 19. Large working resistance support

- (4) Through the arrangement of an intelligent mine pressure monitor, comprehensive and continuous monitoring of mine pressure characteristics of the working face (weighting step, weighting strength, sustained period, support load change), especially in the middle and upper area, the roof movement range and intensity are large, easy to fall, support toppling, extrusion, accurate prediction of roof weighting time is crucial. The probability of roof caving can be reduced by increasing the advancing speed of the working face (greater than 3 m/d) and reducing the mining height (about 3.5 m).

7. Conclusions

- (1) The roof failure and migration characteristics of large mining height face are more active than those of general mining height in steeply dipping coal seams. The dip angle affects the slip-filling characteristics of caved gangue. The rolling and filling degree of caving gangue is considerably higher than that of the gently inclined coal seam, and the range of the free surface area increases, which provides a large space for the failure and movement of the middle and upper main roof strata in the inclined working face. Cross-layer, large-scale, and asymmetrical multilevel spatial ladder-like rock structure forms easily. The breaking of the main roof can easily result in the formation of an anti-dip pile structure, and its instability will form a greater degree of impact pressure on the middle and upper area.
- (2) Due to the influence of the dip angle effect, the deformation and failure of the surrounding rock and the filling form show obvious asymmetric characteristics. The roof stress relief arch is an 'inverted spoon' shape. With the increase of dip angle, the stress release arch decreases, the length of the gangue support area increases, and the height of the caving zone decreases. The filling form of gangue evolves from trapezoid → triangle → rectangle + triangle, and the three-dimensional unbalanced constraint effect of gangue filling body on the roof and floor strata becomes apparent, and the deformation failure area develops to the upper part of the working face.

- (3) Influenced by gangue along the working face inclination and lateral slide filling, a free surface is formed in the middle and upper area, and the gangue filling exhibits nonuniformity in the inclination and advancing direction, which results in the load and deformation failure characteristics of the roof, and the basic form of surrounding rock structure formed after the failure also exhibit considerable differences along the inclination and advancing direction.
- (4) The mine pressure law revealed the characteristics of unbalanced sub-regions, and the working resistance in the middle area of the working face is the largest, followed by the upper area and the lower area. With the increase in the dip angle, the stability of roof strata in the lower area was enhanced, and the space, amplitude, and intensity of roof strata movement in the middle and upper areas increased. The load of the support is changeable, and the interaction between the supports increased considerably. The contact state of the support-surrounding rock system is poor, which results in dynamic instability and induces the surrounding rock disaster.

Acknowledgment

This work was supported by the National Natural Science Foundation of the PRC (52174126, 51974227), Major Scientific and Technological Innovation Projects in Shandong Province (2019JZZY020326), Shaanxi Outstanding Youth Science Fund Project (2023-JC-JQ-42) and Shaanxi University Youth Innovation Team Project.

References

- [1] Y.P. Wu, D.F. Yun, P.S. Xie, H.W. Wang, D. Lang, B.S. Hu, Progress, practice and scientific issues in steeply dipping coal seams fully-mechanized mining. *J. China Coal Soc.* **45** (1), 24-34 (2020) (in Chinese).
- [2] Y.P. Wu, K.Z. Liu, D.F. Yun, P.S. Xie, H.W. Wang, Research progress on the safe and efficient mining technology of steeply dipping seam. *J. China Coal Soc.* **39** (8), 1611-1618 (2014) (in Chinese).
- [3] J.H. Wang, Present status and development tendency of fully mechanized coal mining technology and equipment with high cutting height in China. *Coal Sci. Technol.* **34** (1), 4-7 (2006) (in Chinese).
- [4] Y.P. Wu, B.S. Hu, D. Lang, Y.P. Tang, Risk assessment approach for rockfall hazards in steeply dipping coal seams. *Int. J. Rock Mech. Min. Sci.* **138**, 104626 (2021). DOI: <https://doi.org/10.1016/j.ijrmms.2021.104626>
- [5] H.W. Wang, Y.P. Wu, J.Q. Jiao, P.P. Cao, Stability Mechanism and Control Technology for Fully Mechanized Caving Mining of Steeply Inclined Extra-Thick Seams with Variable Angles. *Mining, Metall. Explor.* **38**, 1047-1057 (2021). DOI: <https://doi.org/10.1007/s42461-020-00360-0>
- [6] X.P. Lai, H. Sun, P.F. Shan, M. Cai, J.T. Cao, F. Cui, Structure instability forecasting and analysis of giant rock pillars in steeply dipping thick coal seams. *Int. J. Min. Met. Mater.* **22** (12), 1233-1244 (2015). DOI: <https://doi.org/10.1007/s12613-015-1190-z>
- [7] W.Y. Lv, Y.P. Wu, M. Liu, J.H. Yin, Migration law of the roof of a composited backfilling longwall face in a steeply dipping coal seam. *Minerals* **9** (3), 188. (2019). DOI: <https://doi.org/10.3390/min9030188>
- [8] P.S. Xie, Y. Luo, Y.P. Wu, X.C. Gao, S.H. Luo, Y.F. Zeng, Roof deformation associated with mining of two panels in steeply dipping coal seam using subsurface subsidence prediction model and physical simulation experiment. *Mining Metall. Explor.* **37** (2), 581-591. (2020). DOI: <https://doi.org/10.1007/s42461-019-00156-x>
- [9] H.S. Tu, S.H. Tu, C. Zhang, L. Zhang, X.G. Zhang, Characteristics of the Roof Behaviours and mine pressure manifestations during the mining of steep coal seam. *Arch. Min. Sci.* **62** (4), 871-890 (2020). DOI: <https://doi.org/10.1515/amsc-2017-0060>

- [10] R.A. Frumkin, Predicting rock behaviour in steep seam faces (in Russian). *International Journal of Rock Mechanics and Mining Sciences & Geomechanics Abstracts* **20** (1), A12-A13 (1983). DOI: [https://doi.org/10.1016/0148-9062\(83\)91717-5](https://doi.org/10.1016/0148-9062(83)91717-5)
- [11] Z. Rak, J. Stasica, Z. Burtan, D. Chlebowski, Technical aspects of mining rate improvement in steeply inclined coal seams: A case study. *Resources* **9** (12), 1-16 (2020). DOI: <https://doi.org/10.3390/resources9120138>
- [12] Z.Y. Wang, L.M. Dou, J. He, A.Y. Cao, X.W. Li, P.B. Li, C.S. Wu, Experimental investigation for dynamic instability of coal-rock masses in horizontal section mining of steeply inclined coal seams. *Arabian J. Geosci.* **13** (15), 1-14 (2020). DOI: <https://doi.org/10.1007/s12517-020-05753-5>
- [13] G.Z. Yin, X.S. Li, W.B. Guo, Photo-elastic experimental and field measurement study of ground pressure of surrounding rock of large dip angle working coalface. *Chin. J. Rock Mech. Eng.* **29** (S1), 3336-3343 (2010). (in Chinese).
- [14] Y.P. Wu, P.S. Xie, H.W. Wang, S.G. Ren, Incline masonry structure around the coal face of steeply dipping seam mining. *J. China Coal Soc.* **35** (8), 1252-1256 (2010). (in Chinese).
- [15] J. Zhang, J.N. Liu, Y.J. Wang, G. Yang, S.L. Hou, Y.J. Wang, M.C. He, J. Yang, Study on pressure relief mechanism of hydraulic support in working face under directional roof crack. *Arch. Min. Sci.* **68** (1), 103-123 (2023). DOI: <https://doi.org/10.24425/ams.2023.144320>
- [16] H.W. Wang, Y.P. Wu, M.F. Liu, J.Q. Jiao, S.H. Luo, Roof-breaking mechanism and stress-evolution characteristics in partial backfill mining of steeply inclined seams. *Geomat. Nat. Hazard. Risk.* **11** (1), 2006-2035 (2020). DOI: <https://doi.org/10.1080/19475705.2020.1823491>
- [17] P.S. Xie, Y.P. Wu, Deformation and failure mechanisms and support structure technologies for goaf-side entries in steep multiple seam mining disturbances. *Arch. Min. Sci.* **64** (3), 561-574 (2019). DOI: <https://doi.org/10.24425/ams.2019.129369>
- [18] J.A. Wang, J.L. Jiao, Criteria of support stability in mining of steeply inclined thick coal seam. *Int. J. Rock Mech. Min. Sci.* **82**, 22-35 (2016). DOI: <https://doi.org/10.1016/j.ijrmm.2015.11.008>
- [19] S.Y. Chen, Q. Lv, Y. Yuan, Key Technologies and its Application of Gob-Side Entry Retaining by Roof Cutting in a Deep Mine. *Arch. Min. Sci.* **68** (1), 103-123 (2023). DOI: <https://doi.org/10.24425/ams.2023.144320>
- [20] S.H. Luo, T. Wang, Y.P. Wu, C.Y. Tian, D. Lang, H.T. Zhao, Space-time evolution characteristics of stress transfer path of surrounding rock in longwall mining of steeply dipping seam. *J. China Coal Soc.* **47** (07), 2534-2545 (2022). (in Chinese).
- [21] J.A. Wang, J.W. Zhang, X.M. Gao, J.D. Wen, Y.D. Gu, Fracture mode and evolution of main roof stratum above longwall fully mechanized top coal caving in steeply inclined thick coal seam (I) – initial fracture. *J. China Coal Soc.* **40** (6), 1353-1360 (2015). (in Chinese).
- [22] W.Y. Lv, Y.P. Wu, M. Liu, J.H. Yin, Migration law of the roof of a composited backfilling longwall face in a steeply dipping coal seam. *Minerals* **9** (3) (2019). DOI: <https://doi.org/10.3390/min9030188>
- [23] P.S. Xie, Y.Y. Zhang, S.H. Luo, J.J. Duan, Instability Mechanism of a Multi-Layer Gangue Roof and Determination of Support Resistance Under Inclination and Gravity. *Mining, Metall. Explor.* **37** (5), 1487-1498 (2020). DOI: <https://doi.org/10.1007/s42461-020-00252-3>
- [24] P. Nguyen, S. Rajwa, M. Płonka, W. Stachura, Geomechanical Assessments of Longwall Working Stability – A Case Study. *Arch. Min. Sci.* **67** (2), 333-354 (2022). DOI: <https://doi.org/10.24425/ams.2022.141462>
- [25] K. Yang, X.L. Chi, S. Liu, Instability mechanism and control of hydraulic support in fully mechanized longwall mining with large dip. *J. China Coal Soc.* **43** (7), 1821-1828 (2018). (in Chinese).
- [26] G.F. Wang, Y.J. Xu, D.Y. Li, Analysis on supporting principle and its application of powered support in large inclined fully mechanized face based on balance of rigid and flexible combined overturning moment. *Chin. J. Rock Mech. Eng.* **37** (S2), 4125-4132 (2018). (in Chinese).
- [27] H.W. Wang, Y.P. Wu, P.S. Xie, Y.J. Li, P.P. Cao, The quantitative filling characteristics of the waste rock and roof movement mechanism in the steeply inclined working face. *J. China Univ. Min. Technol.* **45** (5), 886-892, 922 (2016). (in Chinese).
- [28] Y.C. Yin, J.C. Zou, Y.B. Zhang, Y. Qiu, K. F. D.M. Huang, Experimental study of the movement of backfilling gangues for goaf in steeply inclined coal seams. *Arabian J. Geosci.* **11** (12), (2018). DOI: <https://doi.org/10.1007/s12517-018-3686-0>